

# IONOSPHERIC CORRECTION METHOD FOR PRECISE POSITIONING WITH GPS ACTIVE NETWORK

GAO Shan, CHEN Wu, HU Cong-wei, CHEN Yong-qi, DING Xiao-li

(Department of Land Surveying and Geo-Informatics,

The Hong Kong Polytechnic University, Kowloon, Hong Kong, P. R. China)

**Abstract:** The ionospheric delay error is a major error source which degrades the positioning accuracy in network real time kinematic (RTK) positioning over a long distance. Different approaches are proposed to estimate GPS errors based on GPS reference network, such as virtual reference stations (VRSs) and network corrections. A new method is used to model the ionospheric total electronic content (TEC) distribution in space. Unlike most ionospheric models, only the ionospheric delays along the satellite tracks are modelled. Therefore, the models are of high precise resolution of the ionospheric TEC distribution in both spatial and temporal scales. A new algorithm is used to solve the equation singularity problem. Experiments demonstrate that the new ionospheric correction method can be used to describe the ionospheric variation at a low latitude area where ionospheric activities are strong. Also, the accuracy of the ionospheric model is enough to support centimeter-level positioning within the network. As ionospheric models are satellite-based models (each satellite has one model), the model parameters can be easily incorporated with the existing differential GPS Radio Technical Commission for Maritime Service (DGPS RTCM) 104 format.

**Key words:** GPS; ionospheric model; precise positioning

**CLC number:** V 249

**Document code:** A

**Article ID:** 1005-1120(2005)02-0107-08

## INTRODUCTION

It is well known that major GPS errors, such as ionospheric, tropospheric delays and orbit errors, are spatially correlated. Pseudorange-based differential GPS (DGPS) and wide area DGPS (WADGPS) have been extensively studied and routinely used for the high precision navigation. The main difference between DGPS and WADGPS is that DGPS provides a total error estimation, while WADGPS separates GPS errors in different sources. On the other hand, most GPS positioning with carrier phases is based on double difference (DD) operation to cancel out common GPS errors between two GPS receivers. Since late 1980s, real time kinematic (RTK) positioning technique has been developed based on DD observations. The key to the success of RTK technique is to reduce GPS errors to a level that integer na-

ture of ambiguities can be reserved. However, along with the increase of distance between two GPS receivers (a few tens kilometers or more), the DD operation cannot cancel out GPS errors, especially orbit errors, ionospheric and tropospheric delays, and conventional RTK technique cannot be directly applied<sup>[1,2]</sup>.

In recent years, network RTK technique has been studied by many research groups, aiming at developing a centimeter-level accuracy RTK system for a long distance to reference stations<sup>[3-5]</sup>. Different approaches have been studied, such as network correction<sup>[3,6]</sup> and VRS technique<sup>[7,8]</sup>. They have been well reviewed<sup>[9]</sup>. In general, the network RTK algorithms can be divided into three steps: firstly, the ambiguities between the reference stations have to be resolved on their integers; and then the residuals from reference sta-

**Foundation item:** Supported by the Hong Kong RGC (PolyU 5075/01E and PolyU 5062/02E) Projects.

**Received date:** 2005-01-19; **revision received date:** 2005-05-25

**E-mail:** lsw@chen@polyu.edu.hk Journal Electronic Publishing House. All rights reserved. <http://www.cnki.net>

tions are used to generate error models; finally, the errors are interpolated to the user locations<sup>[1]</sup>. Usually the interpolation algorithms are separately applied to the dispersive (ionosphere) and the non-dispersive (geometric) errors. Another approach is presented in Ref. [6]. As the major error over long baselines is the ionospheric delay, a tomographic ionospheric model generated by the reference stations is used to reduce the ionospheric effect on GPS measurements, then conventional RTK technique is used to determine the position of GPS receivers.

In RTK operation, the corrections need to be sent to users in real time. The VRS method requires a dual way communication link. A user sends his location to the network control center. The network control center generates "virtual" GPS observations at a user location and sends the data back to the user. The network correction method broadcasts messages, which can be residuals for each reference station or some model parameters, to all users. Currently, studies are carried out to propose a new format of "network RTK corrections" to integrate into existing Radio Technical Commission for Maritime Service (RTCM) 104 format for DGPS<sup>[10]</sup>. However, the form of network RTK corrections is different from that of DGPS corrections, as DGPS corrections are given for each satellite while network RTK corrections are related to reference stations.

A new way is proposed to model GPS ionospheric delays using a reference network. Unlike most GPS generated ionospheric models in Refs. [11–13] that try to model the ionospheric delays in the whole space, this paper only models the ionospheric delays along the satellite tracks. For each satellite, an ionospheric model is generated and then the model parameters are transmitted to users (similar to the DGPS correction form). The user calculates the ionospheric delays at the point and removes them from GPS measurements. Finally, conventional RTK technique can be used to determine user's position over long baselines as the ionospheric effects are removed from data.

## 1 IONOSPHERIC CORRECTION ALGORITHM

As other network RTK algorithms, the integer ambiguities are firstly resolved between the reference stations within the network.

$DD$  observations for carrier phases  $L_1$  and  $L_2$  are given in Ref. [14]

$$\lambda DD(\Phi) = DD(\rho) + \lambda DD(N_1) - \Delta I_{\text{ion}1} + \Delta T_{\text{Trop}} + \epsilon \quad (1)$$

$$\lambda DD(\Phi) = DD(\rho) + \lambda DD(N_2) - \Delta I_{\text{ion}2} + \Delta T_{\text{Trop}} + \epsilon \quad (2)$$

where the subscripts for stations and satellites are omitted, and 1, 2 are the subscripts identifying for carrier phases  $L_1$ ,  $L_2$ .  $DD$  is the algorithm for "()" ;  $\Phi$  the carrier phase observation (cycle);  $\rho$  the geocentric distance between the station and the satellite (m);  $N$  the carrier phase ambiguity (cycle);  $\lambda$  the wavelength of the phase (m);  $\Delta I_{\text{ion}}$  the  $DD$  ionospheric refraction (m);  $\Delta T_{\text{Trop}}$  the  $DD$  tropospheric delay (m), and  $\epsilon$  the  $DD$  measurement noise (m).

The tropospheric delay may be modeled with the meteorological data and removed from Eqs. (1, 2). The carrier phase ambiguities can be simply calculated if the ionospheric delays are ignored

$$DD(N) = DD(\Phi) - DD(\rho) / \lambda \quad (3)$$

However, due to the ionospheric irregularities, the ionospheric  $DD$  residuals can be much larger than half cycle ( $0.5\lambda$ ). This makes it difficult to directly resolve the ambiguities using Eq. (3). In the algorithm, the widelane ambiguities are firstly solved by combining the carrier phase and pseudorange data. And then  $L_1$  and  $L_2$  ambiguities are determined by the constraint of widelane ambiguities<sup>[15, 16]</sup>.

Widelane ambiguity is

$$DD(N_w) = DD(N_1) - DD(N_2) = DD(\Phi) - DD(\Psi) - DD(\rho) / \lambda_w \quad (4)$$

$L_1$  and  $L_2$  ambiguities are

$$DD(N_1) = \frac{f_1}{f_w} DD(\Phi) - \frac{f_2}{f_w} (DD(\Psi) + DD(N_w)) - \frac{DD(\rho)}{f_w} \quad (5)$$

$$DD(N_2) = DD(N_1) - DD(N_w) \quad (5)$$

A single shell ionospheric model is then used to represent the ionospheric delays. The slant total electronic content (*STEC*) is calculated by the product of the vertical total electronic content (*VTEC*) and a mapping function<sup>[14]</sup>

$$STEC = map(\theta) \cdot VTEC$$

$$map(\theta) = \left[ 1 - \left( \frac{R \cdot \cos\theta}{R + H} \right)^2 \right]^{-0.5} \quad (6)$$

where  $\theta$  is the satellite elevation angle;  $R$  the mean radius of the earth and  $H$  the assumed shell height of the ionosphere.

The basic observations in the estimation equation for ionospheric *TEC* are geometry-free combination observations<sup>[17]</sup>

$$\Phi_+ - \Phi_- = \alpha \cdot I_+ + (\lambda_1 N_1 - \lambda_2 N_2) + \overline{2} \epsilon =$$

$$\alpha \cdot \frac{40.28 \cdot STEC}{f_1^2} + (\lambda_1 N_1 - \lambda_2 N_2) + \overline{2} \epsilon \quad (7)$$

$$P_4 = P_2 - P_1 = \alpha \cdot I_+ + c \cdot (D_2 - D_1) + \overline{2} \delta =$$

$$\alpha \cdot \frac{40.28 \cdot STEC}{f_1^2} + IFB + \overline{2} \delta \quad (8)$$

where  $\alpha = \frac{(f_1^2 - f_2^2)}{f_2^2}$  is a constant, and IFB the inner-frequency bias of instruments on the pseudo-range.  $P_1$  and  $P_2$  are pseudo-range measurements for  $L_1$  and  $L_2$  bands;  $\Phi_+$  and  $\Phi_-$  the carrier phase measurements;  $N_1$  and  $N_2$  the ambiguities;  $\Phi_+$  and  $P_4$  the geometry-free combinations for the carrier phase and the pseudo-range, and  $\epsilon$  and  $\delta$  the observation noises for the carrier phase and the pseudo-range, respectively. The subscript and superscript for stations and satellites are omitted. This assumes that the inner-frequency bias of the carrier phase and the multipath between the two frequencies can be neglected.

In order to separate *TEC* and observation biases (ambiguities and inner-frequency biases), Eq. (6) is replaced in Eqs. (7, 8) and *VTEC* is modeled by a Taylor series for each satellite at the ionosphere pierce points (IPPs). The Taylor series model is expressed as<sup>[11]</sup>

$$VTEC = \sum_{n=0}^{n_{\max}} \sum_{m=0}^{m_{\max}} E_{nm} (B - B_0)^n (L - L_0)^m \quad (9)$$

where  $n_{\max}$  and  $m_{\max}$  are the maximum degrees of the two-dimensional Taylor series expansion in latitude  $B$  and in sun-fixed longitude  $L$ ;  $E_{nm}$  ( $n =$

$1, \dots, n_{\max}$ ,  $m = 1, \dots, m_{\max}$ ) the unknown coefficients of the Taylor series; and  $B_0$  and  $L_0$  the coordinates of the origin of the development.

Due to the complexity of the ionospheric *TEC* distribution, this simple single shell model cannot describe the ionospheric distribution in the whole space. In this paper, the Taylor series is used to model the ionospheric *TEC* distribution along every satellite track separately within a very short time span ( $< 1$  min). However, if the ionospheric model parameters  $E_{nm}$  are directly solved, the ambiguities and the inner-frequency bias for each satellite will be mathematically difficult. Firstly, in order to model the *TEC* distribution precisely, the time span of GPS observation has to be short (30 s). With such a short period, both map function values and the observations may change very little. Let the coefficient matrix of the observation equation be near singular. Secondly, as the ambiguity and the bias cannot be precisely estimated due to the singular observation equation, there may exist large biases among the ionospheric models for different satellites. Finally, if the ionospheric model parameters are estimated for every short period, the continuity of ionospheric *TEC* is destroyed.

In order to solve these problems, the strong constraints are firstly introduced by using *DD* ambiguities obtained from Eq. (5). Then the ambiguities in Eq. (7) are solved for the initial period. As ambiguities are constant if satellites are continuously observed, we only need to estimate them when new satellites appear or cycle slips occur. After the ambiguities are solved, they are removed from Eq. (7), and then only ionospheric model parameters need to be estimated.

After the ionospheric model parameters are estimated for each satellite, they can be broadcasted to users. Then users calculate *TEC* values for each satellite using Eqs. (6, 9) and remove the ionospheric effects from observation data. Finally, conventional GPS data processing methods (i.e., static, fast static, RTK) can be applied, with either single frequency or dual frequency receivers.

## 2 EXPERIMENT WITH HONG KONG GPS ACTIVE NETWORK

In order to evaluate the performance of the proposed algorithm, GPS observations on March 4, 2001 from Hong Kong GPS active network are used. Currently, there are six reference stations (HKFN, HKKT, HKLT, HKSL, HKST and HKKY) in the network (as shown in Fig. 1) with the station spacing of 10–15 km. Although the spacing of the network is reasonably small, there are strong ionospheric variations in space, due to the fact that Hong Kong locates at a low latitude area (latitude  $22^\circ$  or geomagnetic latitude  $12^\circ$ ). Fig. 2 shows the  $DD$  residuals of carrier phase  $L_1$  observations with a 9.6 km baseline. It can be seen that the residuals can reach up to 20 cm during daytime, which is even worse than a 100 km baseline in mid-latitude areas<sup>[2, 17–19]</sup>.

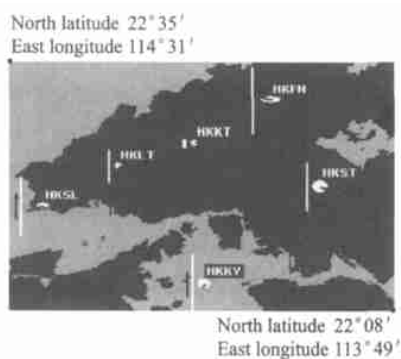


Fig. 1 General picture of HK permanent GPS network of multiple reference stations

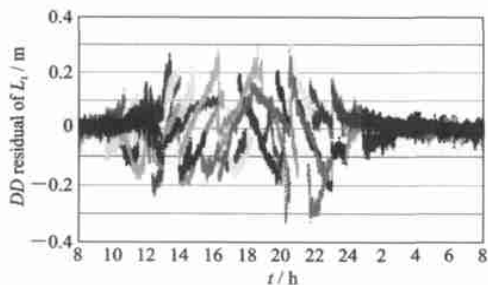


Fig. 2  $DD$  Residuals for carrier phase  $L_1$  (baseline HKKT–HKLT,  $L = 9.6$  km)

processing, every 15 min of observations are used to give one solution. The main problem with such large positioning errors is that the ambiguities cannot be fixed. Fig. 4 shows the success rate when ambiguities are fixed to the integers. It is clear that the success rate of the ambiguity resolution is only 45% for a whole day.

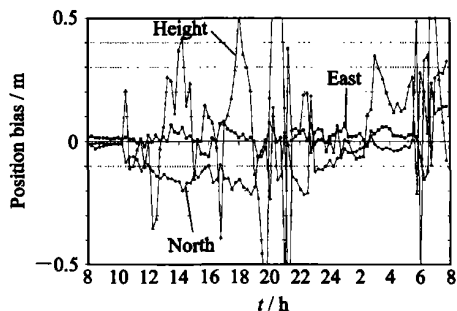


Fig. 3 Positioning error for every 15 min over 24 h (baseline HKKT–HKLT)

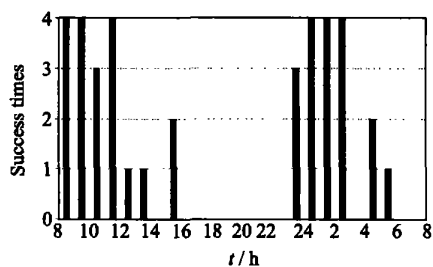


Fig. 4 Success time of ambiguity resolution for every hour (baseline HKKT–HKLT)

In data processing, five stations (except for HKKT in the network) are firstly used to estimate the ionospheric  $TEC$  values along satellite tracks. Both the first order (the linear model) and the second order (the square model) of Taylor series (Eq. (9)) are used, and the square model is slightly better to fit with GPS data. Fig. 5 illustrates the estimated slant ionospheric delays in  $L_1$  for each satellite. In the algorithm, both spatial and temporal changes of ionospheric delays can be clearly distinguished. For example, around sunset (6–9 pm locally), we can see the ionospheric behaviors of wave type. They are typical in low latitude areas where there exist strong ionospheric activities after sunset<sup>[18, 21]</sup>. Fig. 6 shows the residuals of  $L_4$  observation (Eq. (7)) for all used five stations and they are well within 2 cm.

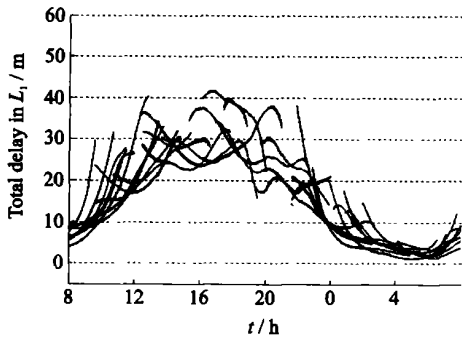


Fig. 5 Ionospheric delays on frequency  $f_1$  for different satellites (different lines denote the ionospheric delays for different satellites)

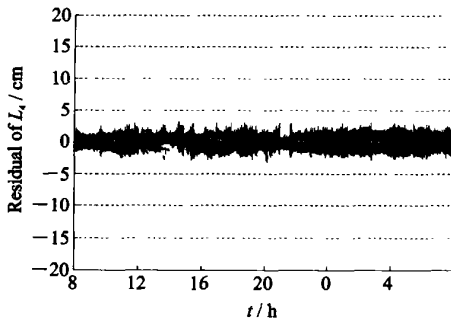


Fig. 6 Residual of  $L_4$ (for all stations)

After the ionospheric delays are determined, models are used to remove the ionospheric delays in all stations. In order to compare the results with the previous case that ionospheric delays are not removed, the double difference fast static method is used to solve the baselines HKLT and HKKT, with every 15 min data for the whole day. Both linear and square ionospheric models are used in the experiment.

Figs. 7, 8 show the success rate of ambiguity resolution when the two models are used to GPS data in the period and the models are estimated. For the square model, except for two periods, the ambiguities can be fixed to their correct integers, and the positioning errors are within a few centimeters with fixed ambiguities (as shown in Fig. 9). For the linear model, there are four periods that the ambiguities cannot be fixed to integers (see Fig. 8). Most of these periods, when the ambiguities cannot be fixed, are happen at the sunset when strong ionospheric activities exist (as shown in Fig. 5).

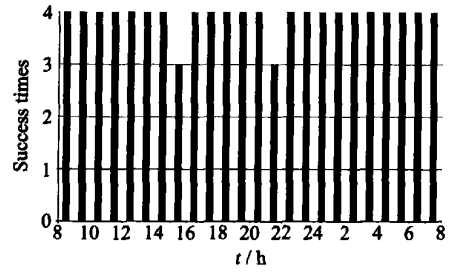


Fig. 7 Success time of ambiguity resolution per hour with the square model's ionospheric correction by interpolation

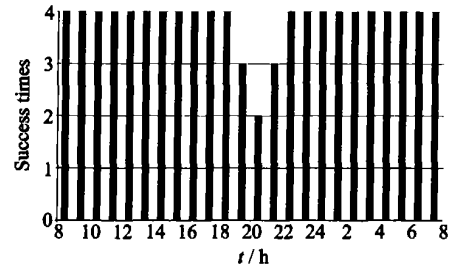


Fig. 8 Success time of ambiguity resolution per hour with the linear model's ionospheric correction by interpolation

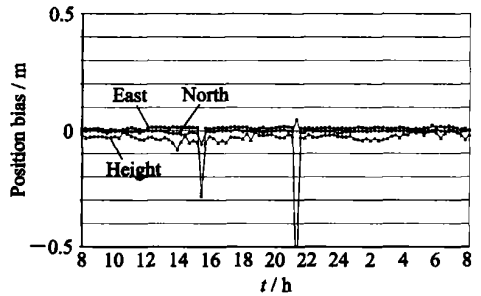


Fig. 9 Positioning error in HKKT with the square model's ionospheric correction by interpolation algorithm

For real time applications, the ionospheric delays need to be predicted to future time. In order to examine the prediction accuracy of the ionospheric models, the first 30 s data are used to generate the models and then used to correct GPS observation data of the next 30 s. Figs. 10, 11 show the success rate of ambiguities resolution during the fast static positioning for the same baseline before using the prediction method. It is shown in Fig. 10 that during daytime to sunset, the success rate of ambiguity with the square model is very poor. However, the linear model

prediction gives the same results as before (compared Fig. 11 with Fig. 8). Thus, for a real time application, the linear model is better than the square model. However, the linear model is difficult to describe the periods when strong ionospheric variation exists.

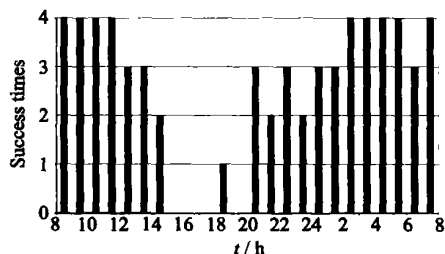


Fig. 10 Success times of ambiguity resolution per hour with the square model's ionospheric correction by extrapolation

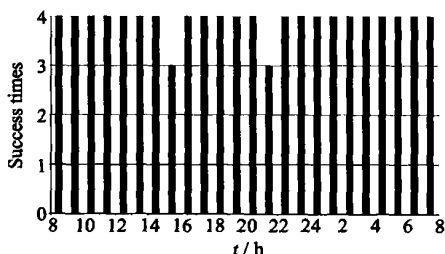


Fig. 11 Success times of ambiguity resolution per hour with the linear model's ionospheric correction by extrapolation

The precise point positioning (PPP) method is used to evaluate the quality of the ionospheric model obtained from the proposed method. The observation model for PPP is described as follows<sup>[22, 23]</sup>

$$\lambda_1 \Phi_1 = \rho + \lambda_1 \cdot N_1 + c \cdot dt + T - I/f_1^2 + \epsilon_1 \quad (10)$$

$$\lambda_2 \Phi_2 = \rho + \lambda_2 \cdot N_2 + c \cdot dt + T - I/f_2^2 + \epsilon_2 \quad (11)$$

$$L_3 = \frac{f_1^2}{f_1^2 - f_2^2} \lambda_1 \Phi_1 - \frac{f_2^2}{f_1^2 - f_2^2} \lambda_2 \Phi_2 = \left[ \rho + c \cdot dt + T + \left( \lambda_1 N_1 - \frac{f_2^2}{f_1^2} \lambda_2 N_2 \right) \right] \frac{f_1^2}{f_1^2 - f_2^2} + \epsilon_3 \quad (12)$$

where  $c$  is the speed of light (m/s);  $f$  the frequency (Hz);  $dt$  the clock offset of satellite and receiver (m);  $T$  the tropospheric delay (m);  $I$  the ionosphere refraction (m), and  $N$  the carrier

phase integer ambiguity (cycle).

Firstly, ionosphere-free combination observations are used (Eq. (12)) to estimate the position of station HKKT by using the PPP method. The position errors are plotted in Fig. 12. It can be seen that the position errors are within a few centimeters after an initial convergent period of about 1 h. Then the ionospheric models obtained by the reference network are used to remove the ionospheric delays in observations of HKKT and  $L_1$  observations (Eq. (9)) are used to calculate the position of HKKT again. The positioning errors with this method are shown in Fig. 13. Compared Fig. 12 with Fig. 13, the positioning errors

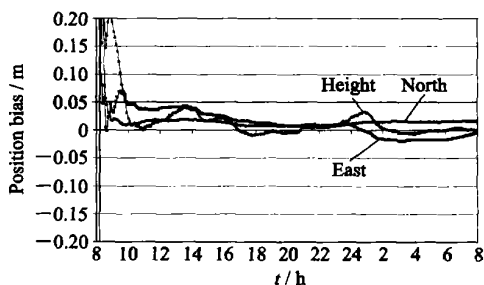


Fig. 12 PPP positioning errors in HKKT by ionosphere-free observations

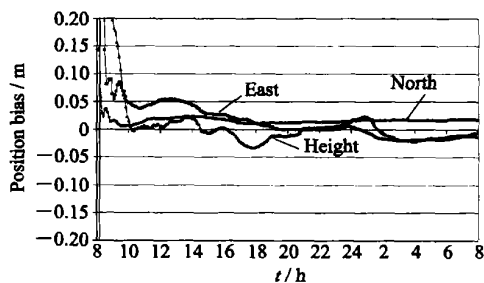


Fig. 13 PPP positioning errors in HKKT by carrier phase  $L_1$  observations with the linear models ionospheric corrections

with these two cases are quite similar. In Fig. 12 the ionospheric effect is removed by the combination of two frequencies and in Fig. 13 by the ionospheric models estimated by the reference network. This indicates that ionospheric models are accurate enough to support centimeter positioning accuracy even with a low cost single frequency receiver.

### 3 CONCLUSIONS

In this paper, a new method is developed to precisely model GPS ionospheric delays by using a GPS reference network. By modeling the ionospheric *TEC* along every satellite track and piecewise along each track, the new ionospheric models can be used to describe high resolution ionosphere variations in both spatial and temporal scales. The experiments demonstrate that the model is accurate to describe the ionospheric variations in low latitude areas where large spatial and temporal ionospheric variations exist.

We also demonstrate that the new ionospheric models are accurate enough to support centimeter GPS positioning. The linear and the square models are compared with experimental data. The results show that the square model has a better fitting to GPS data, but performs poorly on prediction. Therefore, for real time application, the linear model should be used.

As the models are satellite-based, it can be easily incorporated with existing RTCM 104 format for DGPS correction transmission. For each satellite ID, just simply add five parameters for a linear model at the end of DGPS range and range rate corrections. As the ionospheric models only need to be transmitted every 30 s or so, the data quantity to be transmitted is not significantly increased.

With the proposed accurate ionospheric models, the precise point positioning with single frequency GPS receiver is possible. However, the convergent time is still quite long. How to further reduce the convergent time to support single frequency RTK or fast static positioning is need to be studied in future.

#### ACKNOWLEDGEMENT

We thank Lands Department, Hong Kong for providing the data of HK GPS active network.

#### References:

[1] Gao Y, Li Z, McLellan J. Carrier phase based regional area differential GPS for decimeter-level positioning and navigation [A]. Proc 10th Int Tech

Meeting Satellite Division Inst Navigation [C]. Kansas City, Mo, 1997. 1305– 1313.

- [2] Colombo O, Hernandez-Pajares M, Juan J M, *et al.* Resolving carrier phase ambiguities on the fly, at more than 100 km from nearest reference site, with the help of ionospheric tomography[A]. Proc 12nd Int Tech Meeting Satellite Division US Inst Navigation[C]. TN, 1999. 1635– 1642.
- [3] Lachapelle G, Alves P, Fortes L, *et al.* DGPS RTK positioning using a reference network [A]. Proc 13rd Int Tech Meeting Satellite Division US Inst Navigation[C]. Salt Lake City, USA, 2002. 1165– 1171.
- [4] Dai L, Han S, Wang J. A study on GPS/GLONASS multiple reference station technique for precise real-time carrier phase-based positioning[A]. Proc 14th Int Tech Meeting Satellite Division Inst Navigation [C]. Salt Lake City, USA, 2001. 392– 403.
- [5] Wammomger L. Real-time differential GPS error modelling in regional reference station networks[J]. IAG Scientific Assembly. Brazil: Springer, 1997, 76 (7): 86– 92.
- [6] Cannon M E, Lachapelle G. The use of multiple reference station VRS for precise kinematic positioning [A]. Proc Japan Institute of Navigation, GPS Symposium[C]. Tokyo, Japan, 2001.29– 37.
- [7] Cruddace P, Wilson I, Euler H J, *et al.* The long road to establishing a national network RTK solution [A]. Proc FIG XXII Int Conf [C]. Washington, USA, 2002.
- [8] Hu G, Khoo H. Development and assessment of GPS virtual reference stations for RTK positioning [J]. Journal of Geodesy, 2003, 77(4): 292– 302.
- [9] Fotopoulos G, Cannon M. An overview of multi-reference station methods for cm-level positioning[J]. GPS Solution, 2002, 4(3): 1– 10.
- [10] Trimble. Network RTK format proposal for RTCM-SC104 Version 3.0[R]. RTCM Paper 006-2002-SC104-281.
- [11] Wild U. Ionosphere and geodetic satellite systems [A]. Permanent GPS Tracking Data for Modelling and Monitoring, Geodätisch-geophysikalische Arbeiten in der Schweiz[C]. Band Schweiz, 1994.
- [12] Schaer S. Mapping and predicting the earth's ionosphere using the global positioning system[A]. Geodätisch-geophysikalische Arbeiten in der Schweiz, Schweizerische Geodätische Kommission, Institut für Geodäsie und Photogrammetrie, Eidg. Technische Hochschule-Zürich[C]. Zürich, Switzerland,

1999, 59.

- [13] Hugentobler U, Schaer S, Fridez P. The documentation of the bernese GPS software version 4.2[D]. Astronomical Institute, University of Berne, Switzerland, 2001.
- [14] Hofmann-Wellenhof B, Lichtenegger H, Collins J. Global positioning system: theory and practice [M]. Fourth Revised Edition. New York: Springer-Verlag, Wein, 1997.
- [15] Sun H, Cannon M, Melgard T. Real-time GPS reference network carrier phase ambiguity resolution [A]. Proc Nat Tech Meeting Inst Navigation[C]. San Diego, CA, 1999. 193- 199.
- [16] Chen W, Hu C, Ding X, *et al.* Rapid static and kinematic positioning with Hong Kong GPS active network[A]. 14th International Technical Meeting of the Satellite Division of the Institute of Navigation-ION-2001[C]. Salt Lake City, USA, 2001. 11- 14.
- [17] Teunissen P J G, Kleusberg A. GPS for geodesy [M]. Second Revised Edition. New York: Springer-Verlag, 1998.
- [18] Chen W, Gao S, Hu C, *et al.* Effects of ionospheric scintillations on GPS observations in low latitude area [A]. Proceedings of 2003 Int Symposium on GPS/GNSS[C]. Tokyo, Japan, 2003. 339- 346.
- [19] Gulyaeva T. Regional analytical model of ionospheric total electron content: monthly mean and standard deviation[J]. Radio SCI, 1999, 34(6): 1507 - 1512.
- [20] Horemuz M, Sjöberg L. Rapid GPS ambiguity resolution for short and long baselines[J]. Journal of Geodesy, 2002, 76: 381- 391.
- [21] Dabas R. Ionosphere and its influence on radio communications[J]. Resonance, India, 2000.
- [22] Chayangkoon B. Elements of GPS precise point positioning[D]. Augusta: University of Maine, 2000.
- [23] Heroux P, Kouba J. GPS precise point positioning using IGS orbit products[J]. Physics and Chemistry of the Earth Part - A: Solid Earth and Geodesy, 2001, 26(6- 8): 573- 578.

## 高精度 GPS 定位的精密电离层模型

高山, 陈武, 胡丛伟, 陈永奇, 一晓利  
(香港理工大学土地测量及地理资讯学系, 香港九龙, 中国)

摘要: 在长距离 GPS 实时动态定位 (RTK) 过程中, 电离层延迟误差是影响定位精度的主要误差源。目前, 由于采用全空间电离层模型精度不够, 对长距离 RTK 定位主要采用双差电离层残差内插方式。本文提出一种新的电离层模型。该模型仅对每个卫星轨迹通过的电离层部分进行建模, 可适用于高精度 GPS 定位。采用香港数据, 结果表明,

该模型可较好地模拟低纬度电离层变化, 并可支持 GPS 厘米级定位精度。

关键词: GPS; 电离层模型; 精密定位

中图分类号: V 249